Derivation and characterization of chimera-competent eXtra-Embryonic eNdoderm (XEN) cells from pig blastocysts

Chi Park[1,2]*, Young Jeoung[1,2], Jun Uh[3], Kieun Park[1,2,4], Jessica Bridge[1,2], Anne Powell[2,4], Jie Li[5,6,7,8], Laramie Pence[1,2], Tianbin Liu[6,7,8], Hai-Xi Sun[6,7,8], Ying Gu[6,7,8], Yue Shen[5,6,7,8,9], Jun Wu[10,11], Juan-Carlos Izpisua Belmonte[12,*], and Bhanu P. Telugu[1,2,4]*

[1]Animal and Avian Sciences, University of Maryland, College Park, MD 20742;
[2]Animal Bioscience and Biotechnology Laboratory, USDA, ARS, Beltsville, MD 20705;
[3]Department of Animal and Poultry Sciences, Virginia Polytechnic Institute and State University, Blacksburg, VA 24061;
[4]RenOVAte Biosciences Inc, Reisterstown, MD 21136;
[5]BGI Education Center, University of Chinese Academy of Sciences, Shenzhen 518083, China
[6]BGI-Shenzhen, Shenzhen, 518083, China
[7]Guangdong Provincial Key Laboratory of Genome Read and Write, Shenzhen, 518120, China
[8]Guangdong Provincial Academician Workstation of BGI Synthetic Genomics, BGI-Shenzhen, Guangdong, China
[9]Shenzhen Engineering Laboratory for Innovative Molecular Diagnostics, Shenzhen, 518120, China.
[10]Department of Molecular Biology, University of Texas Southwestern Medical Center, Dallas, TX 75390;
[11]Hamon Center for Regenerative Science and Medicine, University of Texas Southwestern Medical Center, Dallas, TX 75390
[12]Salk Institute, La Jolla, San Diego, CA 92037

Keywords: primitive endoderm, stem cell, chimera, XEN, SCNT

***Correspondence**: E-mail: chpark@umd.edu; belmonte@salk.edu; and btelugu@umd.edu.

Lead contact: btelugu@umd.edu

Abstract

We report for the first time, the derivation and characterization of extra-embryonic endoderm (XEN) cells from primitive endoderm (PrE) of porcine (p) embryos. The pXEN cells can be reliably and reproducibly generated from in vitro, in vivo and parthenote embryos, and expressed canonical PrE- and XEN-specific markers (*GATA4*, *GATA6*, *SOX17*, *SALL4*, *FOXA2*, and *HNF4A*). Transcriptome analysis of pXEN cells confirmed their XEN cell origin. When injected into blastocyst stage embryo, the pXEN cells contributed to wide-spread chimerism including visceral yolk sac, chorion, as well as embryonic gut and liver primordium in the fetus. The pXEN cells were shown to be an efficient nuclear donor for generating cloned offspring. Taken together, pXEN cells fulfill a longstanding need for a stable, chimera-competent, and nuclear transfer-compatible porcine embryonic cell line with applications for genome editing in livestock.

Introduction

In mammals, delamination of primitive endoderm (PrE) from the inner cell mass (ICM) in the late blastocyst-stage embryo marks the second fate specification event (the first being the separation of trophectoderm (TE) from the ICM). The PrE differentiate into visceral endoderm (VE) and parietal endoderm (PE) that line ICM and TE, respectively (Cockburn & Rossant, 2010). Together, the VE and PE generate the yolk sac, the first placental membrane. The yolk sac serves as the main placenta in rodents until mid-gestation (d11.5), and performs several important functions including providing nutritional support, gas exchange, hematopoiesis, and patterning cues to the developing embryo. However, in non-rodent species including pig and humans, the yolk sac is short-lived (Bauer *et al*, 1998; Carter, 2016). Regardless, in all species the PrE does not contribute to the embryonic endoderm, which emerges later following gastrulation (Kwon *et al*, 2008).

In culture, three types of stem cells can be established from the mouse embryo: embryonic stem cells (ESC) from the EPI, trophoblast stem cells (TSC) from TE, and XEN cells from PrE, which contribute to the embryo proper, the placenta, and the yolk sac, respectively (Rossant, 2008). The XEN cells can also be induced from ESC by overexpression of PrE-specific genes, *Gata-4, 6* (Fujikura *et al*, 2002; Wamaitha *et al*, 2015), or *Sox17* (McDonald *et al*, 2014), or by treatment with growth factors (Cho *et al*, 2012). More recently, naïve extraembryonic endodermal cells (nEnd) resembling the blastocyst-stage PrE-precursors have been developed from the authentic mouse ESC (Anderson *et al*, 2017). In rat, XEN cells established from blastocysts have different culture requirements and gene expression profiles compared to mouse XEN cells

(Debeb *et al*, 2009; Galat *et al*, 2009). While mouse XEN cells mainly contribute to the PE (Lin *et al*, 2016) in chimeras, rat XEN cells contribute to the VE (Galat *et al*, 2009). It is unclear whether XEN cells from non-rodent animals (human and pig) have potency similar to mouse or rat (Seguin *et al*, 2008). In this regard, the pig model can prove to be uniquely valuable in bridging the translational gap between rodents and humans.

Authentic ESC from pigs (p) have yet to be generated even after three decades of extensive investigation. The major reason for difficulties in the derivation of pESC is the instability of the pluripotent state (Alberio *et al*, 2010; Telugu *et al*, 2010). Even though derivation of pESC from EPI cells has proven to be difficult, extraembryonic (ExE) cells within the early blastocyst outgrowths grow rapidly and outnumber the EPI cells, which can often be misinterpreted as epiblast cells (Keefer *et al*, 2007). There are several reports describing pig EPI-like cells with properties similar to human ESC (Hou *et al*, 2016; Xue *et al*, 2016). However, these observations are purely conjectural, only fulfilling minimal criteria of pluripotency, and lacking the deterministic *in vivo* demonstration of pluripotency (Ramos-Ibeas *et al*, 2018; Xue *et al*, 2016). Besides ESC, attempts to establish TSC and XEN cells from pig or other domestic animals has received little attention, and requires more stringent assays to identify their potential (Ezashi *et al*, 2011; Shen *et al*, 2019).

Here we describe the establishment of XEN cells from the PrE of pig blastocysts. To-date these pXEN cells represent the only well characterized embryo-derived stem cell line that can be readily and reproducibly established under current culture conditions. The pXEN cells are stable in culture, undergo self-renewal for extended periods of time, contribute predominantly to the yolk sac and at a minor level to

embryonic endoderm (gut) in chimeras, and can serve as nuclear donors to generate live offspring.

Results

In vitro derivation and expansion of primary PrE outgrowths

A central assumption behind the failure to establish pESC is a rapid loss of pluripotency in primary outgrowths (Alberio *et al*, 2010), however no details of lineage identities during the derivation phase have been given. We therefore aimed at clarifying cellular identity in the early blastocyst outgrowth. Whole blastocyst explants following attachment became flattened and spread out within 2 days of culture (Figure 1a). As primary outgrowths expanded, TE cells began to first emerge and then underwent dramatic morphological changes, becoming larger and flatter, and soon-after undergoing apoptosis (Figure 1a). After 5 days, a population of round and dispersed epithelial cells emerged as a discrete cell layer bordering the ICM (hereafter called "EPI") cells (Figure 1a). The majority of EPI cells were SOX2 positive (18/21) but only a few co-expressed NANOG (4/21) (Figure 1b), similar to the staining pattern observed in the blastocyst (Figure 1c). Notably, the large round cells initially considered as TE cells, stained positive for GATA6 (9/12) and CK18 but lacked CDX2 expression (Figure 1b). The expression of GATA4, a later marker of the PrE, was also detected in few small round cells (4/7) (Appendix Figure s1a), confirming two distinct PrE progenitors expressing GATA factors in primary outgrowths. Of these subpopulations, small and large PrE were distinguishable based on cell morphology and by their expression of CK18 (Appendix Figure s1b). Although initial explants could be established from early blastocysts (day 5-6), late blastocysts (fully expanded or hatched, day 7-8) with discernable ICM and TE lineages (Figure 1c; Appendix Figure s1c), established stable PrE populations (Figure 1d and e) and were used further in our studies.

Initially, NANOG or GATA4 positive (+) cells were mostly undetectable, but cytoplasmic GATA4 expression appeared in the periphery of the early ICM outgrowths by day 3 of culture (Figure 1f). Intriguingly, NANOG/GATA4 co-positive cells that lined the side of EPI outgrowths gradually increased by 5 days, and by day 7, > 90% of GATA4+ cells co-expressed NANOG (Figure 1f). In contrast, the expression of NANOG was detected in few if any EPI cells, while the SOX2 expression was progressively decreased with time, indicating the loss of pluripotency (Appendix Figure 1d; Figure 1e and g). Besides GATA factors, SALL4 (Lim *et al*, 2008) a key stemness marker of XEN cells was expressed in the nuclei of PrE cells which had a small and compacted appearance. A large fraction (~75%) of SALL4+ cells had nuclear foci of intense histone 3 lysine 27 trimethylation (H3K27me3), a hallmark of the inactive X in female outgrowths (Rugg-Gunn *et al*, 2010). Consistent with this observation, XIST levels were 2-fold higher in SALL4+ PrE cells than in EPI cells (Figure 1i). This reflects the lineage specific dynamics of H3K27me3 accumulation on the X-chromosome, and could be the consequence of the co-expression of *SALL4* (Lim *et al*, 2008).

Cellular properties and molecular signature of pig XEN cells

Self-renewal of XEN cells is dependent on *Sall4* expression (Lim *et al*, 2008). The emergence of a distinct SALL4+ PrE population in primary outgrowths has prompted us to attempt derivation of pXEN cells. After 7-9 days of culture, PrE cells began to emerge in primary outgrowths and could be clearly demarcated based on their morphology and their easy dissociation from the EPI cells (Appendix Figure s2a). Both EPI and PrE colonies displayed a distinct morphology following serial passages (Figure

2a). Consistent with previous findings, the EPI colonies underwent spontaneous differentiation toward a fibroblast- or neuron-like appearance by passages 5-7. The colonies from PrE-derivatives, on the other hand, were more stable in culture. The colonies were propagated as flattened colonies and passaged as clumps by mechanical or enzymatic dissociation (Figure 2b), but did not survive passage as single cells, even when treated with ROCK inhibitor Y-27632 (Figure 2b; Appendix Figure s2b). Following sub-passage, the PrE colonies initially appeared as a homogenous colony of cells and grew as a monolayer. Upon serial passaging, two distinct populations emerged; a cobble-stone morphology in the center of the colony, and epithelial sheet-type cells at the borders of the colony (Appendix Figure s2c). The cells at the periphery were strongly alkaline phosphatase (ALP) positive (Figure 2c) and exhibited rapid proliferation as confirmed by PCNA staining (Appendix Figure s2c). The density of the feeder cells influenced the colony stability with the optimal densities ranging from 3- 4 x 10^4 cells per cm^2. Lower feeder densities (< 2 x 10^4 cells/cm^2) resulted in differentiation of cells with the expression of VIMENTIN (Figure 2d), and at high densities (>1 x 10^5 cells/cm^2) the cultures were more closely packed and showed reduced replating efficiency. The cells expressed PrE-specific markers (GATA4, GATA6, SOX17, SALL4, FOXA2, and HNF4A) with no expression of pluripotent markers (OCT4, SOX2, and NANOG) (Figure 2e; Appendix Figure s2e). Notably, NANOG was no longer detected upon passaging indicating a possible role for NANOG only in early PrE specification. While CDX2 is not detectable, other TE-markers EOMES and GATA3 were expressed, consistent with the role of the latter in endodermal specification. Taken together, the molecular signature confirmed the established colonies as XEN cells.

We tested the growth factor requirements of pXEN cells based on observations from mouse (Kunath *et al*, 2005). Withdrawal of either LIF, bFGF or both, had no impact on primary PrE induction. However, in the omission of both, the cells failed to expand into stable cell lines confirming the growth factor responsiveness (Figure 2f). The colonies that arose in LIF or FGF4 alone did not proliferate as rapidly as cells cultured with either bFGF, or both LIF and bFGF (Figure 2g). Omission of both growth factors resulted in a dramatic reduction in colony formation, with low expression of XEN marker genes *FOXa2*, *GATA4*, *GATA6*, *HNF4a*, *PDGFRa*, *SALL4* and *SOX17,* and high expression of VE- (*AFP* and *UPA*), and PE-genes, (*SNAIL*, *SPARC*, and *VIMENTIN*), consistent with spontaneous differentiation (Figure 2h). The XEN cells could be stably maintained in serum-free N2B27-based defined medium with lower degree of cellular differentiation and expression of VE- and PE-related genes, however this resulted in a longer cell doubling time (Appendix Figure s2f and g). One interesting finding is the presence of characteristic lipid droplets in the cytoplasm of pXEN cells (Figure 2a), which readily disappeared when plated in the absence of growth factors or feeder cells with a concomitant loss of SALL4 expression, but no change in EOMES expression (Figure 2i). Although little is known about the mechanisms mediating the presence of lipid droplets, this feature could be leveraged as a non-invasive marker of SALL4+ cells.

Based on these preliminary trials, we established putative XEN cell lines from *in vivo*-developed (vi, n=4), *in vitro*-fertilized (vf, n=13), and parthenogenetically activated (pg, n=14) porcine blastocysts. All lines exhibited stable morphology and marker expression, irrespective of their embryonic origin (Figure 2j). The pXEN cells were maintained with proliferative potential in culture for extended passages (>50 passages),

and were karyotypically normal (Figure. 2k). After 5 days of hanging culture, static embryoid body structures were formed and expressed higher level of differentiated state VE and PE markers (Appendix Figure s2i). Transcriptomic analysis of pXEN cells expressed characteristic XEN cell repertoire and clustered closely with rodent XEN cells (Figure 2l, m, and n). Importantly, no teratoma development was observed in any recipient mice transplanted with 1×10^6 to 10^7 cells from the six robust pXEN cell lines (Appendix Table s2) indicating that all injected pXEN cells were committed and not pluripotent cells.

Contribution of pXEN Cells to Chimeras

Mouse XEN cells contribute to PE, whereas rat XEN cells incorporate into both VE and PE lineages in chimeras (Galat *et al*, 2009; Kunath *et al*, 2005). Given these disparities, we evaluated the properties of pXEN cells in chimera studies (Figure 3a). To facilitate lineage tracing, we generated a transgenic pXEN reporter cell line by knocking-in a constitutive human UBC promoter driven GFP reporter downstream of the pCOL1A1 locus (hereafter, Tg-pCOL1A:GFP) using CRISPR/Cas9 system as previously described (Park *et al*, 2016) (Appendix Figure s3a). Labeled pXEN (Xnt $^{pCOL1A:GFP}$ #3-2) cells were injected as single cells or 5-10 cell clumps into parthenogenetic embryos at the morula (Day 4) or early blastocyst stages (Day 5). Cells injected as clumps integrated into host embryos more efficiently (77.3 to 85.7%) than individual cells (37.5 to 47.4%); and cells injected at the blastocyst stage showed better incorporation into ICM (85.7%) than when injected at the morula stage (77.3%) (Appendix Table s3). To evaluate *in vivo* chimeric development, pXEN cells were

similarly injected as clumps into host blastocysts (n=109). Following overnight culture, the resulting re-expanded blastocysts (n=94) were transferred into 3 recipient sows (Figure 3b). A total of 25 fetuses (27%) were retrieved from 2 recipients on day 21 (Figure 2b). Among the recovered fetuses, the injected GFP^+ cells were found in the yolk sac (6/9) and the fetal membranes (5/9), and a small group of GFP^+ cells were observed in one embryo (1/9) (Figure 3b). Notably, GPF^+ cells extensively contributed to the yolk sac in two chimeras (XeC#2-3 and XeC#2-4) with a moderate signal in the allantochorion (Figure 3c). The GFP^+ cells observed in embryos were from pXEN cells and not due to auto-fluorescence as confirmed by genomic PCR. Quantification of GFP^+ cells by qPCR confirmed XEN cell chimerism at 1.7% in 2 embryos, and at 12.9% in the yolk sac, and 8% in the allantochorion, signifying active integration and proliferation of pXEN cells during embryogenesis (Figure 3d). As shown in Fig. 3e, immunostaining with the anti-GFP antibody identified GFP^+ cells in the embryonic gut of 3 chimeric fetuses (XeC#1-2, XeC #2-3, and XeC #2-6). The GFP^+ donor cell population integrated predominantly into the visceral endodermal layers, but rarely into the outer mesothelial layers or endothelial cells in the yolk sac (Figure 3e middle; Appendix Figure s3c), and to a minor extent populated amnion, allantois, chorion (Figure 3e; Appendix Figure s3d), and gut endoderm (Appendix Table s5). Overall, the chimerism frequency of the pXEN cells was rather high (60%).

Generation of viable cloned offspring from pXEN cells via SCNT

In an effort to test the utility of pXEN cells as nuclear donors, we performed SCNT with the pXEN cells used in the chimera assay (above), alongside previously

published crossbred knock-out fetal fibroblasts (FF $^{NGN3-/-}$) as controls (Sheets *et al*, 2018). A total of 222 cloned embryos reconstituted from pXEN (n=61) and FF (n=161) were co-transferred into two surrogate gilts to exclude confounding variables associated with recipient animals affecting the outcome. Following embryo transfers, one pregnancy was established, and 8 cloned piglets were delivered at term. Three of the 8 piglets were GFP positive and black coated (4.9%) confirming the COL1A:GFP Ossabaw XEN cell origin, while 5 piglets were white coated and GFP negative and therefore from the control fibroblasts (3.1%) (Figure 4a). As expected, the piglets exhibited ubiquitous expression of GFP in all tissues (Figure 4b). The genotype of the offspring was confirmed by PCR (Figure. 4c). In addition to this, we performed multiple rounds of SCNT with FF $^{pCOL1A:GFP}$ (#3) from which the XEN cells were derived. Despite being genetically identical, no offspring were obtained from founder GFP fibroblasts, but the XEN cells derived from fibroblasts served as efficient donors in SCNT.

Discussion

Despite all efforts made so far, establishment of embryo-derived stem cells without major chemical intervention in pigs has largely been unsuccessful. As shown by multiple groups, the EPI fraction of primary explants fails to proliferate, and the cultures are rapidly overtaken by proliferating ExE cells. That said, there were no published reports that temporally followed the fate of the ExE derived lines in culture, nor have they been adequately characterized. However, the equivalent lines from mouse have been thoroughly characterized. This report for the first time takes a systematic and in-depth look at the derivation, establishment, and characterization of XEN cells from PrE.

During early mouse embryo development, NANOG is expressed in EPI cells and excluded from GATA4^{+} PrE cells in embryo (Chazaud *et al*, 2006; Plusa *et al*, 2008). This seems counterintuitive given the mutual antagonism between NANOG and GATA4 that facilitates key cell-fate decisions between EPI and PrE, respectively (Mitsui *et al*, 2003). Indeed, several lines of evidence support the expression of NANOG in pig hypoblast (Gao *et al*, 2011; Kobayashi *et al*, 2017), which is contrary to the mouse model. Emergence of the PrE population with co-expression of GATA4/NANOG appears to represent an early step in PrE specification, highlighting mechanistic differences in early lineage specification between mouse and pig. That said, the establishment of pXEN cells, their culture characteristics, and the resulting molecular signatures (including high expression of *FOXa2*, *GATA4*, *GATA6*, *HNF4a*, *PDGFRa*, *SALL4* and *SOX17*) are shared with rodent models, with the exception of failure to establish XEN cells in FGF4-based medium, and intolerance to dispersal as single cells.

Generation of embryonic chimeras has been considered the most stringent test

of stem cell differentiation potential *in vivo* (Mascetti & Pedersen, 2016). This study demonstrates that despite the lack of pESC, it is possible to generate embryo-derived stem cell lines with PrE-like properties as confirmed by lineage-restricted plasticity in the resulting chimeras, which were not irrevocably fixed (e.g., yolk sac, placenta, gut endoderm) (Kwon *et al*, 2008). This indicates that the pXEN cells are in a less committed endodermal naïve state. In the pig, freshly isolated ICMs are capable of widespread tissue contribution, including germline colonization in chimeras (Nagashima *et al*, 2004). Despite this, the pluripotent EPI or iPS cells were preferentially engrafted into extraembryonic tissues (Ezashi *et al*, 2011; Fujishiro *et al*, 2013; West *et al*, 2010). It is likely that in the absence of defined conditions, embryonic outgrowths are unstable and transition to a XEN-like state (Zhao *et al*, 2015). Future chimera trials will be performed in embryos that lack key gate-keeper genes (for e.g., SALL4), where the relative contribution of pXEN cells to embryonic and ExE endodermal lineages are expected to be higher when compared to current experiments performed with wild type embryos.

In vivo generation of human organs via interspecies chimeras between human and pigs via blastocyst complementation has been acknowledged as a source of donor organs for life-saving regenerative medicine applications (Kobayashi *et al*, 2010; Matsunari *et al*, 2013; Wu *et al*, 2017). Evidence gathered in the present study demonstrates the engraftment potential of pXEN cells with lineage restricted cell fate. When such experiments are performed with human XEN cells, the potential contribution to endodermal organs will provide an on-demand source of human endodermal cells in pig hosts. Our present findings make the use of pXEN cells a particularly attractive

choice to generate tissue-specific chimeras for endodermal organs, while limiting unwanted contribution to undesirable organs (e.g., germ cell or neural lineage) in interspecies chimeras- a likely outcome with the use of ESC/iPS cells (Masaki *et al*, 2016; Rashid *et al*, 2014).

Another advantage of the pXEN cells is the competency to generate live animals via SCNT. This is especially attractive in complex genome editing and genetic engineering applications where a long-life span in culture is desirable. As evidenced from this study, genetically modified fibroblast cells failed to generate live offspring, whereas, the pXEN cells derived following cloning of the FFs were able to generate live offspring at a relatively high efficiency (4.9%). One potential explanation is the epigenetic disruption caused by transfection that may have compromised embryonic development. It's possible that the pXEN cell derivation process resets the genome to a state that allows full-term development. It remains to be seen if this could be applicable to other cells which fail to generate live offspring. Taken together, we argue that the derivation of pXEN cells fulfils a longstanding need in the livestock genetics field for a stem cell line of embryonic origin that can be reliably and reproducibly generated, are stable in culture, have the potential to contribute to chimeras, and are a good source for creating cloned animals.

Methods

Experimental Animal Assurance

All experiments involving live animals were performed in accordance with the approved guidelines of the Beltsville ARS and Thomas D. Morris Inc., Institutional Animal Care and Use Committee (IACUC). All experimental protocols involving live animals were approved by the IACUC committee.

Establishment and maintenance of pig XEN cells

All chemicals were purchased from Sigma-Aldrich (St. Louis, MO), unless noted otherwise. Embryonic explants and XEN cells were cultured on a feeder layer of early passage (n=3) CF-1 mouse embryonic fibroblasts (MEF) cells mitotically inactivated by treatment with mitomycin-C (3 hr, 10 µg/mL). A day before seeding the embryos or XEN cells, the feeders were plated in MEF medium based on high-glucose Dulbecco's modified Eagle medium (DMEM; Gibco, Grand Island, NY) supplemented with 10% (v/v) fetal bovine serum (FBS; HyClone Laboratories Inc., Logan UT, USA) on 0.1% (v/v) gelatin-coated four-well plates (Nunclon, Roskilde, Denmark) at a density of 3-5 × 10^5 cells per cm^2. At least 2 hr before the start of the experiment, the MEF medium was aspirated and replaced with ‘standard ES medium’ which included DMEM/ Nutrient Mixture Ham's F12 (DMEM/F-12; Gibco) supplemented with 15% ES-qualified fetal calf serum (FCS; HyClone Laboratories Inc.), 1 mM sodium pyruvate, 2 mM L-glutamine, 100 units/mL penicillin-streptomycin, 0.1 mM 2-β-mercaptoethanol, 1% non-essential amino acids (NEAA; all from Gibco), with various combination of growth factors; 10 ng/mL human recombinant leukemia inhibitory factor (hrLIF; Milipore, Bedford, MA) and 10 ng/mL human recombinant basic fibroblast growth factor (hrbFGF; R&D Systems,

Minneapolis, MN). Other media combinations that were tested include RPMI 1640 or N2B27 serum free medium (1:1 ratio of DMEM/F12 and Neurobasal medium plus N2 and B27, all from Gibco), with a combination of 5 ng/mL LIF and/or 10 ng/mL bFGF, or 25 ng/mL human recombinant fibroblast growth factor 4 (hrFGF4; R&D Systems) and 1 µg/mL heparin (Niakan *et al*, 2013). Following initial plating, attachment and outgrowth development, the medium was refreshed on d 3, followed by media exchange every 2 days. After 7-8 days of culture, the primary outgrowths were mechanically dissociated into small clumps, and transferred onto fresh feeders for passaging. The pXEN cells were cultured at 38.5°C in 5% O_2 and 5% CO_2, with the culture medium being refreshed every other day and passaged at 1:20 every 7-8 days. Cells were passaged as clumps by gentle pipetting following 10 min digestion with Accutase (Gibco)**.** Before routine passaging and freezing, cells were cultured with Rho Kinase (ROCK) inhibitor Y-27632 (10 µM; StemCell Technologies, Vancouver, Canada) at least 2 hr prior to dissociation (Watanabe *et al*, 2007). Each XEN cell line was frozen in FBS based medium supplemented with 8% (v/v) DMSO and recovered with high viability. In order to determine chromosomal stability in long term culture, cytogenetic analysis was performed by Cell Line Genetics.

Alkaline phosphatase staining

The cells were fixed with 4% (w/v) paraformaldehyde for 3 min at room temperature (RT) and were washed three times with DPBS. Alkaline phosphatase (ALP) staining was performed with a BCIP/NBT Alkaline Phosphatase Color Development Kit following the manufacturer's instructions. The cells were examined using an inverted microscope.

In vitro differentiation of XEN cells into parietal or visceral endoderm:

The pXEN cells were differentiated by means of embryoid body (EB) formation as previously described (Chuykin *et al*, 2013). pXEN cells were dissociated as clumps, washed, and resuspended in medium (DMEM/F12 plus 15% FBS) as hanging drops on the lid of a 60 mm dish, and cultured for 5 days, during which time spheroids were formed.

Methods for embryo production and manipulation

The *in vivo* and *in vitro* embryo production were performed as described previously (Park *et al*, 2016; Sheets *et al*, 2018). For generating parthenote, *in vitro* fertilized embryos, and for performing somatic cell nuclear transfer (SCNT), cumulus-oocyte complexes were purchased from a commercial supplier (DeSoto Biosciences, Seymour, TN, USA). After *in vitro* maturation, the cumulus cells were removed from the oocytes by gentle pipetting in a 0.1% (w/v) hyaluronidase solution. Briefly, for *In vitro* fertilization (IVF), pre-diluted fresh semen (Duroc; Progenes) was centrifuged twice at 200 g for 3 min in DPBS containing 0.2% BSA. The sperm pellet was adjusted to a concentration of 2×10^5 sperm per mL and co-incubated with matured oocytes in modified Tris-buffered medium containing 0.4% BSA for 5 hr in a humidified atmosphere (5% CO_2 in air). Following three washes, putative zygotes were cultured and maintained in PZM3 medium in a low oxygen air (5% O_2 and 5% CO_2 in air). For obtaining *in vivo* embryos, donor animals were synchronized using Regumate and artificially inseminated at 12 and 24 hr following the observation of first standing estrus. On days 5-7 post-insemination, *in vivo* embryos were recovered by flushing oviduct with 35 ml of TL-Hepes buffer containing 2% BSA under general anesthesia. For SCNT, fetal fibroblasts (FF) were

synchronized to the G1/G0-phase by serum deprivation (DMEM with 0.2% FCS) for 96 hr, and pXEN cells were mitotically arrested by serum free medium (N2B27 with 1% BSA) for 48 hr followed by incubation with aphidicolin (0.1 μM) for 12 hr. Enucleation was performed by aspirating the polar body and the MII metaphase plates using a micropipette (Humagen, Charlottesville, VA, USA) in 0.1% DPBS supplemented with 5 μg/mL of cytochalasin B. After enucleation, donor cells were placed into the perivitelline space of an enucleated oocyte. Fusion of cell–oocyte couplets was induced by applying two direct current (DC) pulses (1-sec interval) of 2.1 kV/cm for 30 μs using a ECM 2001 Electroporation System (BTX, Holliston, MA). After fusion, the reconstituted oocytes were activated by a DC pulse of 1.2 kV/cm for 60 μs, followed by post-activation in 2 mM 6-dimethylaminopurine for 3 hr. After overnight culture in PZM3 with a histone deacetylase inhibitor Scriptaid (0.5 μM), the cloned embryos were surgically transferred into the oviduct. Parthenogenetic embryos were produced by the activation procedures used for SCNT.

Embryo Transfer

The surrogate recipients were synchronized by oral administration of progesterone analog Regumate for 14-16 days. Animals in natural estrus on the day of surgery were used as recipients for SCNT embryo transfers (into oviduct), and at days 5-6 after natural heat were used for blastocyst transfer (into uterus) for generating chimeras. Surgical procedure was performed under a 5% isofluorane general anesthesia following induction with TKX (Telazol 100 mg/kg, ketamine 50 mg/kg, and xylazine 50 mg/kg body weight) administered intramuscularly. Pregnancies were confirmed by ultrasound

on day 27 following transfer. Cloned piglets were delivered at day 117 of pregnancy by natural parturition.

RNA and DNA preparations

For isolation of genomic DNA (gDNA) from cells and tissues, the QIAamp mini DNA Kit (Qiagen, Valencia, CA, USA) was used according to the manufacturers' instructions. Total RNA was isolated using Trizol plus RNeasy mini kit (Qiagen) and mRNA from individual blastocysts was extracted using the Dynabeads mRNA Direct Kit (Dynal Asa, Oslo, Norway). Synthesis of cDNA was performed using a High Capacity cDNA Reverse transcription kit (Applied Biosystems; ABI,Foster City, CA) according to the manufacturers' instructions. The QIAseq FX Single Cell RNA Library kit (Qiagen) was used for Illumina library preparation and transcriptomics analysis.

qPCR: Relative quantification of mRNA levels was carried out using SYBR Green technology on an ABI 7500 Fast Real-Time PCR system (Applied Biosystems). The thermal-cycling conditions are: 20 s at 95°C followed by 40 cycles of 3 s at 95°C and 30 s at 60°C. The primers were designed to yield a single product without primer dimerization. The amplification curves for the selected genes were parallel. All reactions were performed from three independent biological and two technical replicates. Two reference genes, ACTB and YWHAG were used to normalize all samples and the relative expression ratios were calculated via the $2^{-\Delta\Delta Ct}$ method (Livak & Schmittgen, 2001). The primers used in qPCR are listed in Appendix Table s1.

Data access

A total of 12 RNA-seq data sets generated in this study have been deposited in the CNSA (https://db.cngb.org/cnsa/) of CNGBdb with accession code CNP0000388, and

also NCBI Gene Expression Omnibus (GEO; http://www.ncbi.nlm.nih.gov/geo) under accession number GSE128149.

Transcriptomics Analysis

RNA-seq reads were mapped to the pig reference genome (Sscrofa11.1) using HISAT2(Kim *et al*, 2015) (version 2.0.4) with parameters “hisat2 --sensitive --no-discordant --no-mixed -I 1 -X 1000” and to the reference cDNA sequence using Bowtie2 (Langmead *et al*, 2009) with parameters “bowtie2 -q --sensitive --dpad0 --gbar 99999999 --mp 1,1 --np 1 --score-min L,0,-0.1 -I 1 -X 1000 --no-mixed --no-discordant-p 1 -k 200”. Then the expression levels of each gene were calculated by the fragments per kilobase of exons per million fragments mapped (FPKM) using RSEM (Li & Dewey, 2011) with parameters “rsemcalculate-expression --paired-end -p 8” based on the result of Bowtie2. The data of mouse and rat XEN cells were downloaded from GSE106158 (Zhong *et al*, 2018) (mouse: GSM2830587, GSM2830588 and GSM2830589; rat: GSM2830591, GSM2830592 and GSM2830593) and the gene expression levels were calculated in the same way (the mouse and rat reference genome used were GRCm38.p6 and Rnor_6.0, respectively). The expression levels of mouse nEnd were downloaded from GSE10742 (Song *et al*, 2008) (GSM271163, GSM271164 and GSM271165). Then the expression levels of all samples were combined to obtain the expression matrix. Final expression matrix was calculated by cross-species gene expression analysis as reported previously (Gafni *et al*, 2013). The expression values from mouse, rat and pig were transformed separately into relative abundance values: for each gene, the relative abundance value is the expression value divided by the mean of expression values within the same gene across samples in the same species.

The final expression matrix was subjected to hierarchical clustering using R software. Development stage (PE, PrE, TE, VE and EPI)-specific genes were selected to do the subsequent analyses. They were mapped to the final expression matrix to do the PCA and heatmap analysis with R software.

Immunofluorescence and Immunohistochemical analysis

The embryos, explants and derived pXEN cell lines (Xvv#9 and Xnt pCOL1A:GFP#3-2) have been characterized by staining for markers by immunofluorescence (IF) analyses. Samples were fixed with 4% (w/v) paraformaldehyde for 5 min, then washed with DPBS. The sections were permeabilized in DPBS containing 0.01% Triton X-100 (PBT) for 20 min, blocked in blocking solution (10% FBS and 0.05% Triton X-100 in DPBS) for 1 hr, and then incubated with primary antibodies overnight at 4°C. The following day, the sections were washed three times in PBT, followed by incubation in the blocking solution with fluorescence labelled secondary antibodies (Alexa Fluor 488 (1: 500) and/or Alexa Fluor 568 (1:500) against primary antibody host species) for 1 hr. The cell nuclei were stained with DAPI (Life Technologies) for 5 min in the dark at RT. For Immunohistochemistry, representative samples from the chimeric fetuses including fetal membranes were fixed with 4% formalin overnight at 4°C. Serial paraffin sections were prepared by American Histolabs Inc. (Gaithersburg, MD) and stained with hemotaxylin and eosin to serve as a reference. Immunostaining was subjected to heat-induced antigen retrieval at 95-98 °C for 20 min in Tris EDTA buffer (pH 9.0, 0.05%Tween20), cooled at RT for 20 min, permeabilized in DPBS containing 0.01% Triton X-100 (PBT) for 20 min, blocked using Super Block blocking buffer (Thermo Fisher Scientific, Waltham, MA, USA) for 30 min at RT, and incubated with primary and secondary

antibodies and stained using process described above. GFP antibody and IHC protocols were validated with the tissues from a female XEN cloned pig (Xnt clone #1) prior to use in chimera testing. For immunofluorescence and immunohistochemistry, negative control slides, without primary antibody, were included for each experiment to establish background staining. Imaging was performed using an inverted fluorescent microscope (Nikon Eclipse N2000). The source of antibodies used in the experiments were listed in Appendix Table s1.

Generating of a GFP-KI reporter.

In order to establish green fluorescent protein (GFP) gene-based reporter XEN cell line, we used a site-specific knock in (KI) Ossabaw fetal fibroblasts. In order to facilitate KI at high frequencies, we have used a combination of small molecule inhibitor of NHEJ pathway (SCR7) (Maruyama *et al*, 2015) and a pre-complexed Cas9 protein and sgRNA RNP complex to KI a ubiquitous promoter (UBC) driven GFP (Sanger Institute) downstream of a ubiquitously expressed *COL1A1* locus to ensure stable expression of transgenes. After a day of transfection, the GFP-positive (GFP^+) cells were sorted by flow cytometry (Becton Dickinson, Franklin Lakes, NJ, USA) and GFP^+ single cells were replated into wells of a 96-well plate for expansion. After 10–15 days, individual colonies were washed, suspended in 20 µL of lysis buffer (50mM KCl, 1.5mM MgCl2, 10mM Tris pH 8.0, 0.5% NP-40, 0.5% Tween-20 and 100 µg/mL proteinase K) and incubated for 1 h at 65˚C followed by heating the mixture at 95˚C for 10 min to inactivate the enzymes. The cell lysates (2 µL) were directly used as a template for PCR with screening primers (Appendix Table s1). Using this approach, we have identified >60% of the clonal lines showing stable integration of the transgene. The targeted-clones with a strong and

consistent fluorescence intensity as determined by fluorescence microscopy were frozen in 92% FCS and 8% DMSO, prior to use as nuclear donor cells. Using labeled XEN cells, live animals were generated by SCNT.

Chimera assay

For lineage tracing of injected XEN cells, a total of eight reporter XEN cell lines were established from cloned blastocysts (Day 7 to 8), using GFP KI fetal fibroblasts (pCOL1A-GFP #3 and #6). A candidate female XEN cell line (Xnt pCOL1A:GFP#3-2) with stable expression of GFP and XEN markers was used for chimera testing. The cells were pre-treated with Rho Kinase (ROCK) inhibitor Y-27632 (10 μM; StemCell Technologies) for 2 hr and dissociated with Accutase at 38.5 °C for 5 min followed by gentle pipetting. About 3-4 small clumps (10–15 cells) were injected per blastocyst (Appendix Figure s3b). After 20~24 hr of culture, injected blastocysts (n=94) were surgically transferred into the upper part of each uterine horn through needle puncture in recipients at days 5–6 of the estrous cycle (D0=onset of estrus; n=3). On day 15 after embryo transfer, the surrogate animals were euthanized to recover XEN-chimeras (XeC; embryonic day 21). A total of 25 fetuses were obtained after transfer and assessed macroscopically for viability and GFP expression. Fetuses that showed strong GFP expression in yolk sac (XeC#3-4) were cut sagittally; one half was used for histological analysis, whereas the second for DNA extraction. For detecting chimera contribution, gDNA were extracted from three parts of embryos: a small pieces of tissue at the posterior region of the fetus, yolk sac, and allantochorionic membrane. Embryos that were malformed or noticeably delayed (i.e. spherical and ovoid) were used only for gDNA isolation. The gDNA samples were subjected to PCR for chimera detection with

genotyping primers (Appendix Table s1), and qPCR was performed for the detection of knock-in allele and chimerism rate. Prior to use in the qPCR analysis, the dynamic range of qPCR primers were validated (amplification efficiency >90%). The GFP labeled pXEN cell line (Xnt pCOL1A:GFP #3-2) was used as a positive control (GFP^+, 100%) and a non-GFP XEN cell from parthenote embryo (Xpg#1) served as a negative (GFP-, 0%) control for investigating % chimerism. Relative expression was calculated using the comparative $2^{-\Delta\Delta Ct}$ method. qPCR was performed in triplicate. Cycling conditions for both GFP and reference (ACTB and YWHAZ gene) products were 10 min at 95°C, followed by 40 cycles of 95°C for 15 sec, and 60°C for 1 min. The primers used in qPCR are listed in Appendix Table s1.

Teratoma Assay

Immunedeficient-nude (BRG, BALB/c-$Rag2^{null}$ $IL2rg^{null}$; Taconic) and -scid (NIH-III, Cr:NIH-bgnu-Xid; National Cancer Institute) male mice were used to perform teratoma formation assay. Before transplanting, the pXEN cells were incubated for 2 hr in DMEM/F12 supplemented with Y27632 (10 μM). The cells were dissociated mechanically into small clumps, washed and suspended in 0.2 mL of mixture containing equal volumes of DMEM/F12 and Matrigel (Corning, MA, USA)(Prokhorova *et al*, 2009). With six pXEN cell lines, the cell suspensions (1 to 10×10^6 cells) were subcutaneously injected into 6-8-week-old mice (Appendix Table s2). Mice were housed in specific pathogen–free conditions and were monitored for a minimum of 30 weeks.

Statistical analysis

Statistical analysis was performed with GraphPad Prism 6 (GraphPad Software, Inc., San Diego, CA, USA) using two-way analysis of variances (ANOVA) and Tukey's

multiple comparison test at 5% level of significance. Data were presented as mean ± SD.

Acknowledgements: This research was supported by AFRI Grants# 2015-67015-22845 and 2018-67015-27575 from the USDA National Institute of Food and Agriculture, and 1 R01 HD092304-01A1 from NICHD, NIH to BT; Guangdong Provincial Key Laboratory of Genome Read and Write (No. 2017B030301011), Guangdong Provincial Academician Workstation of BGI Synthetic Genomics (No. 2017B090904014), Shenzhen Engineering Laboratory for Innovative Molecular Diagnostics (DRC-SZ[2016]884) and Shenzhen Peacock Plan (No.. KQTD20150330171505310)

Author Contributions: CP, JCB and BT conceived the project and designed the experiments; CP, YJ, YU and JB established and performed characterization of embryonic outgrowths and XEN cells; KP and AP performed the knockin and generated the GFP reporter lines used for generating GFP:XEN cells used in chimera experiments; CP, JL, LP, TL, JS, YG, YS, JW generated the libraries and transcriptomic analysis; CP and BT wrote the initial draft, CP, JW, JCB and BT revised the manuscript based on the input from all authors. All authors approved final draft for submission.

Competing Interests: KP, AP and BT serve as consultants at RenOVAte Biosciences Inc, (RBI). BT is the founding member of RBI. All remaining authors declare no competing or conflicts of interest.

References:

Alberio R, Croxall N, Allegrucci C (2010) Pig epiblast stem cells depend on activin/nodal signaling for pluripotency and self-renewal. *Stem Cells Dev* 19: 1627-36

Anderson KGV, Hamilton WB, Roske FV, Azad A, Knudsen TE, Canham MA, Forrester LM, Brickman JM (2017) Insulin fine-tunes self-renewal pathways governing naive pluripotency and extra-embryonic endoderm. *Nat Cell Biol* 19: 1164-1177

Bauer MK, Harding JE, Bassett NS, Breier BH, Oliver MH, Gallaher BH, Evans PC, Woodall SM, Gluckman PD (1998) Fetal growth and placental function. *Mol Cell Endocrinol* 140: 115-20

Carter AM (2016) IFPA Senior Award Lecture: Mammalian fetal membranes. *Placenta* 48 Suppl 1: S21-S30

Chazaud C, Yamanaka Y, Pawson T, Rossant J (2006) Early lineage segregation between epiblast and primitive endoderm in mouse blastocysts through the Grb2-MAPK pathway. *Dev Cell* 10: 615-24

Cho LT, Wamaitha SE, Tsai IJ, Artus J, Sherwood RI, Pedersen RA, Hadjantonakis AK, Niakan KK (2012) Conversion from mouse embryonic to extra-embryonic endoderm stem cells reveals distinct differentiation capacities of pluripotent stem cell states. *Development* 139: 2866-77

Chuykin I, Schulz H, Guan K, Bader M (2013) Activation of the PTHRP/adenylate cyclase pathway promotes differentiation of rat XEN cells into parietal endoderm, whereas Wnt/beta-catenin signaling promotes differentiation into visceral endoderm. *J Cell Sci* 126: 128-38

Cockburn K, Rossant J (2010) Making the blastocyst: lessons from the mouse. *J Clin Invest* 120: 995-1003

Debeb BG, Galat V, Epple-Farmer J, Iannaccone S, Woodward WA, Bader M, Iannaccone P, Binas B (2009) Isolation of Oct4-expressing extraembryonic endoderm precursor cell lines. *PLoS ONE* 4: e7216

Ezashi T, Matsuyama H, Telugu BP, Roberts RM (2011) Generation of colonies of induced trophoblast cells during standard reprogramming of porcine fibroblasts to induced pluripotent stem cells. *Biol Reprod* 85: 779-87

Fujikura J, Yamato E, Yonemura S, Hosoda K, Masui S, Nakao K, Miyazaki Ji J, Niwa H (2002) Differentiation of embryonic stem cells is induced by GATA factors. *Genes Dev* 16: 784-9

Fujishiro SH, Nakano K, Mizukami Y, Azami T, Arai Y, Matsunari H, Ishino R, Nishimura T, Watanabe M, Abe T, Furukawa Y, Umeyama K, Yamanaka S, Ema M, Nagashima H, Hanazono Y (2013) Generation of naive-like porcine-induced pluripotent stem cells capable of contributing to embryonic and fetal development. *Stem Cells Dev* 22: 473-82

Gafni O, Weinberger L, Mansour AA, Manor YS, Chomsky E, Ben-Yosef D, Kalma Y, Viukov S, Maza I, Zviran A *et al* (2013) Derivation of novel human ground state naive pluripotent stem cells. *Nature* 504: 282-6

Galat V, Binas B, Iannaccone S, Postovit LM, Debeb BG, Iannaccone P (2009) Developmental potential of rat extraembryonic stem cells. *Stem Cells Dev* 18: 1309-18

Gao Y, Jammes H, Rasmussen MA, Oestrup O, Beaujean N, Hall V, Hyttel P (2011) Epigenetic regulation of gene expression in porcine epiblast, hypoblast, trophectoderm and epiblast-derived neural progenitor cells. *Epigenetics* 6: 1149-61

Hou DR, Jin Y, Nie XW, Zhang ML, Ta N, Zhao LH, Yang N, Chen Y, Wu ZQ, Jiang HB, Li YR, Sun QY, Dai YF, Li RF (2016) Derivation of Porcine Embryonic Stem-Like Cells from In Vitro-Produced Blastocyst-Stage Embryos. *Scientific reports* 6: 25838

Keefer CL, Pant D, Blomberg L, Talbot NC (2007) Challenges and prospects for the establishment of embryonic stem cell lines of domesticated ungulates. *Anim Reprod Sci* 98: 147-68

Kim D, Langmead B, Salzberg SL (2015) HISAT: a fast spliced aligner with low memory requirements. *Nat Methods* 12: 357-60

Kobayashi T, Yamaguchi T, Hamanaka S, Kato-Itoh M, Yamazaki Y, Ibata M, Sato H, Lee YS, Usui J, Knisely AS, Hirabayashi M, Nakauchi H (2010) Generation of rat pancreas in mouse by interspecific blastocyst injection of pluripotent stem cells. *Cell* 142: 787-99

Kobayashi T, Zhang H, Tang WWC, Irie N, Withey S, Klisch D, Sybirna A, Dietmann S, Contreras DA, Webb R, Allegrucci C, Alberio R, Surani MA (2017) Principles of early human development and germ cell program from conserved model systems. *Nature* 546: 416-420

Kunath T, Arnaud D, Uy GD, Okamoto I, Chureau C, Yamanaka Y, Heard E, Gardner RL, Avner P, Rossant J (2005) Imprinted X-inactivation in extra-embryonic endoderm cell lines from mouse blastocysts. *Development* 132: 1649-61

Kwon GS, Viotti M, Hadjantonakis AK (2008) The endoderm of the mouse embryo arises by dynamic widespread intercalation of embryonic and extraembryonic lineages. *Dev Cell* 15: 509-20

Langmead B, Trapnell C, Pop M, Salzberg SL (2009) Ultrafast and memory-efficient alignment of short DNA sequences to the human genome. *Genome Biol* 10: R25

Li B, Dewey CN (2011) RSEM: accurate transcript quantification from RNA-Seq data with or without a reference genome. *BMC bioinformatics* 12: 323

Lim CY, Tam WL, Zhang J, Ang HS, Jia H, Lipovich L, Ng HH, Wei CL, Sung WK, Robson P, Yang H, Lim B (2008) Sall4 regulates distinct transcription circuitries in different blastocyst-derived stem cell lineages. *Cell Stem Cell* 3: 543-54

Lin J, Khan M, Zapiec B, Mombaerts P (2016) Efficient derivation of extraembryonic endoderm stem cell lines from mouse postimplantation embryos. *Scientific reports* 6: 39457

Livak KJ, Schmittgen TD (2001) Analysis of relative gene expression data using real-time quantitative PCR and the 2(-Delta Delta C(T)) Method. *Methods* 25: 402-8

Maruyama T, Dougan SK, Truttmann MC, Bilate AM, Ingram JR, Ploegh HL (2015) Increasing the efficiency of precise genome editing with CRISPR-Cas9 by inhibition of nonhomologous end joining. *Nat Biotechnol* 33: 538-42

Masaki H, Kato-Itoh M, Takahashi Y, Umino A, Sato H, Ito K, Yanagida A, Nishimura T, Yamaguchi T, Hirabayashi M, Era T, Loh KM, Wu SM, Weissman IL, Nakauchi H (2016)

Inhibition of Apoptosis Overcomes Stage-Related Compatibility Barriers to Chimera Formation in Mouse Embryos. *Cell Stem Cell* 19: 587-592

Mascetti VL, Pedersen RA (2016) Contributions of Mammalian Chimeras to Pluripotent Stem Cell Research. *Cell Stem Cell* 19: 163-175

Matsunari H, Nagashima H, Watanabe M, Umeyama K, Nakano K, Nagaya M, Kobayashi T, Yamaguchi T, Sumazaki R, Herzenberg LA, Nakauchi H (2013) Blastocyst complementation generates exogenic pancreas in vivo in apancreatic cloned pigs. *Proc Natl Acad Sci U S A* 110: 4557-62

McDonald AC, Biechele S, Rossant J, Stanford WL (2014) Sox17-mediated XEN cell conversion identifies dynamic networks controlling cell-fate decisions in embryo-derived stem cells. *Cell reports* 9: 780-93

Mitsui K, Tokuzawa Y, Itoh H, Segawa K, Murakami M, Takahashi K, Maruyama M, Maeda M, Yamanaka S (2003) The homeoprotein Nanog is required for maintenance of pluripotency in mouse epiblast and ES cells. *Cell* 113: 631-42

Nagashima H, Giannakis C, Ashman RJ, Nottle MB (2004) Sex differentiation and germ cell production in chimeric pigs produced by inner cell mass injection into blastocysts. *Biol Reprod* 70: 702-7

Niakan KK, Schrode N, Cho LT, Hadjantonakis AK (2013) Derivation of extraembryonic endoderm stem (XEN) cells from mouse embryos and embryonic stem cells. *Nat Protoc* 8: 1028-41

Park KE, Park CH, Powell A, Martin J, Donovan DM, Telugu BP (2016) Targeted Gene Knockin in Porcine Somatic Cells Using CRISPR/Cas Ribonucleoproteins. *Int J Mol Sci* 17

Plusa B, Piliszek A, Frankenberg S, Artus J, Hadjantonakis AK (2008) Distinct sequential cell behaviours direct primitive endoderm formation in the mouse blastocyst. *Development* 135: 3081-91

Prokhorova TA, Harkness LM, Frandsen U, Ditzel N, Schroder HD, Burns JS, Kassem M (2009) Teratoma formation by human embryonic stem cells is site dependent and enhanced by the presence of Matrigel. *Stem Cells Dev* 18: 47-54

Ramos-Ibeas P, Nichols J, Alberio R (2018) States and Origins of Mammalian Embryonic Pluripotency In Vivo and in a Dish. *Current topics in developmental biology* 128: 151-179

Rashid T, Kobayashi T, Nakauchi H (2014) Revisiting the flight of Icarus: making human organs from PSCs with large animal chimeras. *Cell Stem Cell* 15: 406-409

Rossant J (2008) Stem cells and early lineage development. *Cell* 132: 527-31

Rugg-Gunn PJ, Cox BJ, Ralston A, Rossant J (2010) Distinct histone modifications in stem cell lines and tissue lineages from the early mouse embryo. *Proc Natl Acad Sci U S A* 107: 10783-90

Seguin CA, Draper JS, Nagy A, Rossant J (2008) Establishment of endoderm progenitors by SOX transcription factor expression in human embryonic stem cells. *Cell Stem Cell* 3: 182-95

Sheets TP, Park KE, Park CH, Swift SM, Powell A, Donovan DM, Telugu BP (2018) Targeted Mutation of NGN3 Gene Disrupts Pancreatic Endocrine Cell Development in Pigs. *Scientific reports* 8: 3582

Shen QY, Yu S, Zhang Y, Zhou Z, Zhu ZS, Pan Q, Lv S, Niu HM, Li N, Peng S, Liao MZ, Wang HY, Lei AM, Miao YL, Liu ZH, Hua JL (2019) Characterization of porcine extraembryonic endoderm cells. *Cell Prolif* 52: e12591

Song JS, Liu X, Liu XS, He X (2008) A high-resolution map of nucleosome positioning on a fission yeast centromere. *Genome research* 18: 1064-72

Telugu BP, Ezashi T, Roberts RM (2010) The promise of stem cell research in pigs and other ungulate species. *Stem Cell Rev* 6: 31-41

Wamaitha SE, del Valle I, Cho LT, Wei Y, Fogarty NM, Blakeley P, Sherwood RI, Ji H, Niakan KK (2015) Gata6 potently initiates reprograming of pluripotent and differentiated cells to extraembryonic endoderm stem cells. *Genes Dev* 29: 1239-55

Watanabe K, Ueno M, Kamiya D, Nishiyama A, Matsumura M, Wataya T, Takahashi JB, Nishikawa S, Nishikawa S, Muguruma K, Sasai Y (2007) A ROCK inhibitor permits survival of dissociated human embryonic stem cells. *Nat Biotechnol* 25: 681-6

West FD, Terlouw SL, Kwon DJ, Mumaw JL, Dhara SK, Hasneen K, Dobrinsky JR, Stice SL (2010) Porcine induced pluripotent stem cells produce chimeric offspring. *Stem Cells Dev* 19: 1211-20

Wu J, Platero-Luengo A, Sakurai M, Sugawara A, Gil MA, Yamauchi T, Suzuki K, Bogliotti YS, Cuello C, Morales Valencia M *et al* (2017) Interspecies Chimerism with Mammalian Pluripotent Stem Cells. *Cell* 168: 473-486 e15

Xue B, Li Y, He Y, Wei R, Sun R, Yin Z, Bou G, Liu Z (2016) Porcine Pluripotent Stem Cells Derived from IVF Embryos Contribute to Chimeric Development In Vivo. *PLoS ONE* 11: e0151737

Zhao Y, Zhao T, Guan J, Zhang X, Fu Y, Ye J, Zhu J, Meng G, Ge J, Yang S, Cheng L, Du Y, Zhao C, Wang T, Su L, Yang W, Deng H (2015) A XEN-like State Bridges Somatic Cells to Pluripotency during Chemical Reprogramming. *Cell* 163: 1678-91

Zhong Y, Choi T, Kim M, Jung KH, Chai YG, Binas B (2018) Isolation of primitive mouse extraembryonic endoderm (pXEN) stem cell lines. *Stem cell research* 30: 100-112

Figure legends

Figure 1. Distinct subpopulations arise from the porcine blastocyst outgrowths.

(a) Phase contrast images depicting morphologies of embryonic outgrowths from days 2 to 5 in culture. In the figure EPI, TE and PrE stands for epiblast, trophectoderm and primitive endoderm, respectively.

(b) Immunostaining for key transcription factors, SOX2 and NANOG (ICM), CDX2 and CK18 (TE), and GATA6 (PrE) in the primary outgrowth at day 3 after explants.

(c) Representative immunofluorescence images of late blastocyst (ICM in dotted circle). In the figure, fraction of cells and percentage of cells that stained positive for NANOG or SOX2 was shown.

(d) The bar graph showing the attachment and outgrowth rates of early and late blastocysts.

(e) Frequencies of SOX2- and GATA6-positive cells in outgrowths. N/D: not detected.

(f) Representative immunostaining (top) and quantitation (bottom) of the number of NANOG or GATA4 positive nuclei in primary outgrowths cultured for 7 days. Open and solid arrows indicate NANOG/GATA4 co- positive and GATA4 positive only cells, respectively.

(g) Representative fluorescence images of CK18 and GATA4 of a Day 7 primary outgrowth (right). Comparison of the transcriptional levels of selected lineage marker genes between PrE cells and EPI cells by qPCR; *, $p<0.05$ according to unpaired *t* test; error bars represent ± SEM (n=3) (left). ACTB was used as an endogenous control.

(h) The expression of H3K27me3 and SALL4 in day 7 primary outgrowth (right). Inset shows the zoom-in of the dashed box. The bar graph showing the quantitation of the

percentage of H3K27me3 focal dots in SALL4 positive or negative cells (left). In all images, nuclei were counterstained with DAPI (blue). Scale bar: 100μm.

(i) The relative XIST mRNA levels in PrE cells compared to EPI cells; *, $p<0.05$ according to unpaired *t* test; error bars represent ± SEM (n=3). ACTB was used as a loading control.

Figure 2. Establishment and characterization of pXEN cells

(a) Representative bright-field images of EPI- derived primary colonies, and PrE-derived XEN cells at passages 3-5.

(b) Efficiency of colony formation of pXEN cells passaged as clumps or single cells. The colony forming activity were greatly impaired when dissociated as single cells. Cells were passaged as clumps by mechanical (clumps-me) or enzymatic dissociation (clumps-en) with Accutase.

(c) Alkaline phosphatase (ALP) staining of an *in vivo*-derived pXEN cells (Xv#9) after culturing for 3 and 7 days.

(d) Representative fluorescence images of VIMENTIN (red) and AFP (green)

(e) Expression of the indicated markers in pXEN at passages 30-35.

(f) Effect of growth factors supplementation on PrE derivation. pXEN cells were seeded onto a 6-well-plate seeded containing a density of 5×10^4 feeder cells per cm^2, and

(g) cell number estimated 48 h following passage. Data are is presented as means ± s.d. (n = 3).

(h) qPCR analyses of total RNA isolated from pXEN cells grown in either the presence or absence of LIF/bFGF for 4 days. ACTB was used as a loading control. The values are represented as mean ± s.d. (n = 3).

(i) Representative images of pXEN cells show the expression of stem cell marker, SALL4 (green) that are significantly reduced in the cells that had lost lipid droplet. Scale bar: 100μm.

(j) qPCR analysis of pXEN cells derived from different embryonic origins. ACTB was used as a loading control. The values are represented as mean ± s.d. (n = 3).

(k) Representative karyotypic analysis of pXEN cell lines, with numbered chromosomes.

(l) RNA-seq analysis of pXEN cells and comparison with analogous derivatives. Data from pig XEN cell lines as well as published data on related cell lines (mouse and rat XEN cells) were included in the comparison. Principal component analysis (PCA) plot of two pXEN cells and other samples. Upper inset shows the color code for each cell type, lower inset shows a separate PCA of only pig vs. mouse vs. rat XEN cells.

(m) hierarchical clustering of pXEN and related samples.

(n)Heatmap comparison of selected XEN-associated extraembryonic endodermal (ExEn) marker gene expression of all samples.

Figure 3. Chimeric contribution of pXEN cells to embryonic and extraembryonic lineages in post-implantation Day 21 embryos.

(a) Schematic representation of the chimera assay.

(b) Table presents a summary of chimera experiments performed by injection of pXEN cells into blastocysts. In the Table, Ys: yolk sac; ExE: extraembryonic membranes; N/D:

not defined (severely retarded fetuses with no fetal or yolk sac parts); and "*" stands for the embryos at the pre-attachment stages (spherical or ovoid).

(c) Representative bright field and fluorescence merged images of normal (XeC#2-3 and XeC#2-4) and retarded (XeC#2-6) fetuses at day 21 of gestation. Yolk sac outlined by the dashed line, and enlarged view of the region marked by the dashed box is shown in the right. In the figure Al stands for allantois; Ch, chorion; Emb, embryo; Ys, yolk sac.

(d) Bar graph representing percent contributions of GFP-XEN in chimeras determined by qPCR; *, $p<0.05$ according to unpaired *t* test; error bars represent ± SEM (n=3).

(e) Representative sagittal or transverse sections of fetuses showing dual immunofluorescence staining for GFP (green) and SALL4 or PECAM1 (red) in embryos; the arrows indicate GFP-positive cells derived from injected pXEN cells in sections. Inset are zoom-in magnified images of the dashed box. Nuclei were stained with DAPI (blue). Al, allantois; Ch, chorion; Emb, embryo; Lp, liver primordium; Pg primitive gut; Ys, yolk sac; Am, amnion; Hp, heart primordium; So, somite. Scale bar: 100μm.

Figure 4. Generation of viable cloned piglets using pXEN or fibroblasts

(a) Summary of SCNT experiments. #Cloning efficiency was obtained by calculating total no. fetuses or piglets / total no. embryos transferred. $data obtained from our previous study. *NGN3$^{-/-}$ cells originated from our previous report[25]. All the fetal fibroblasts and pXEN cells with the exception of NGN3$^{-/-}$ cells used as SCNT donors were derived from the same fetus (female Ossabow fetal fibroblast #6).

(b) Representative images showing 10 days old NGN3 KO white (outbred)- and XEN Black (Ossabow)-coated littermates. The fluorescence images of live GFP+ piglets and

whole organs taken with blue light illumination showing ubiquitous expression of GFP transgene, and confirming the pXEN cell as nuclear donors.

(c) A representative digital gel image of the 1.2-kb amplicon with primers within and outside of the targeting vector confirming site-specific knockin was generated by Fragment Analyzer.

1 **Figure 1**

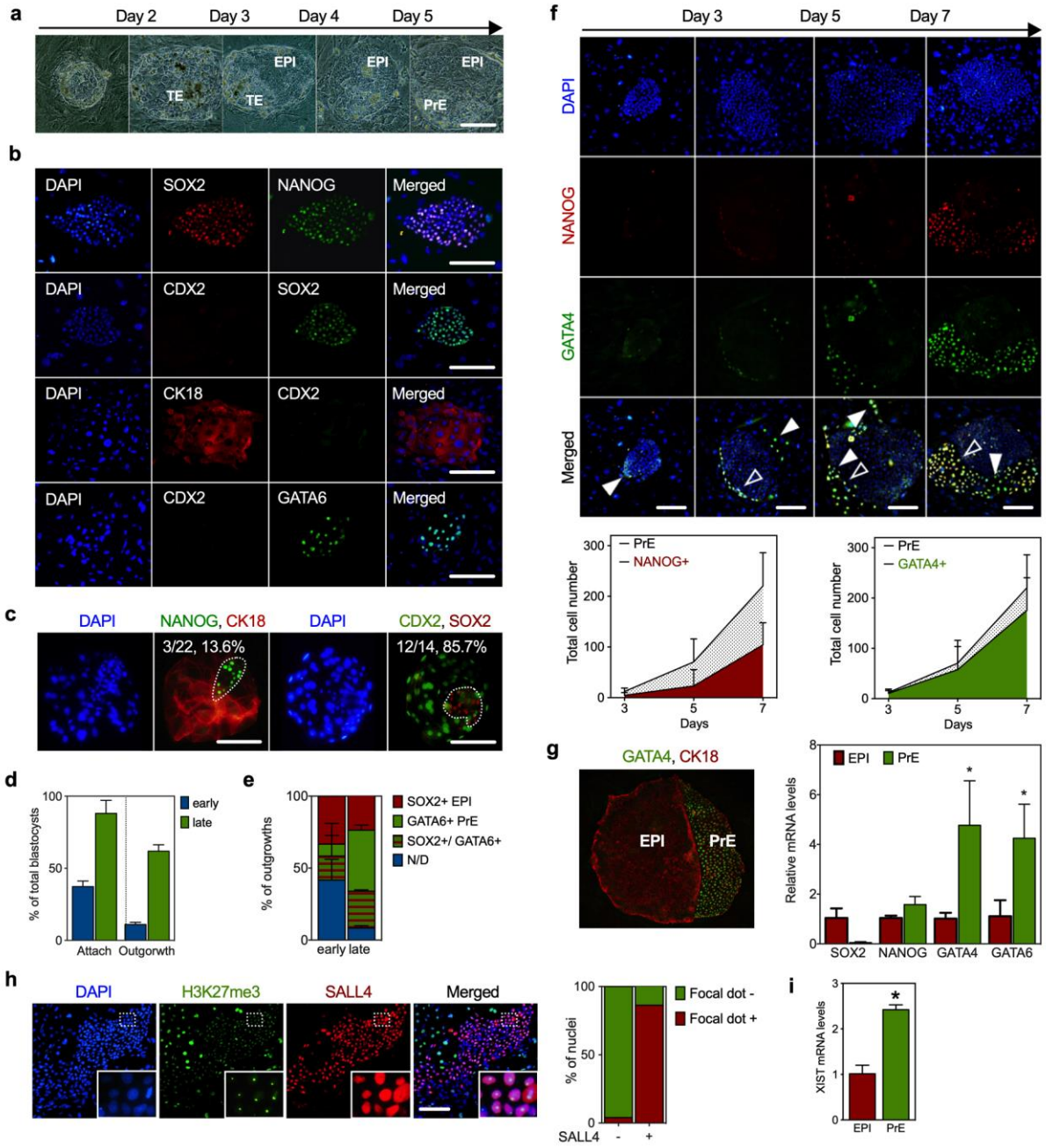

2
3

Figure 2

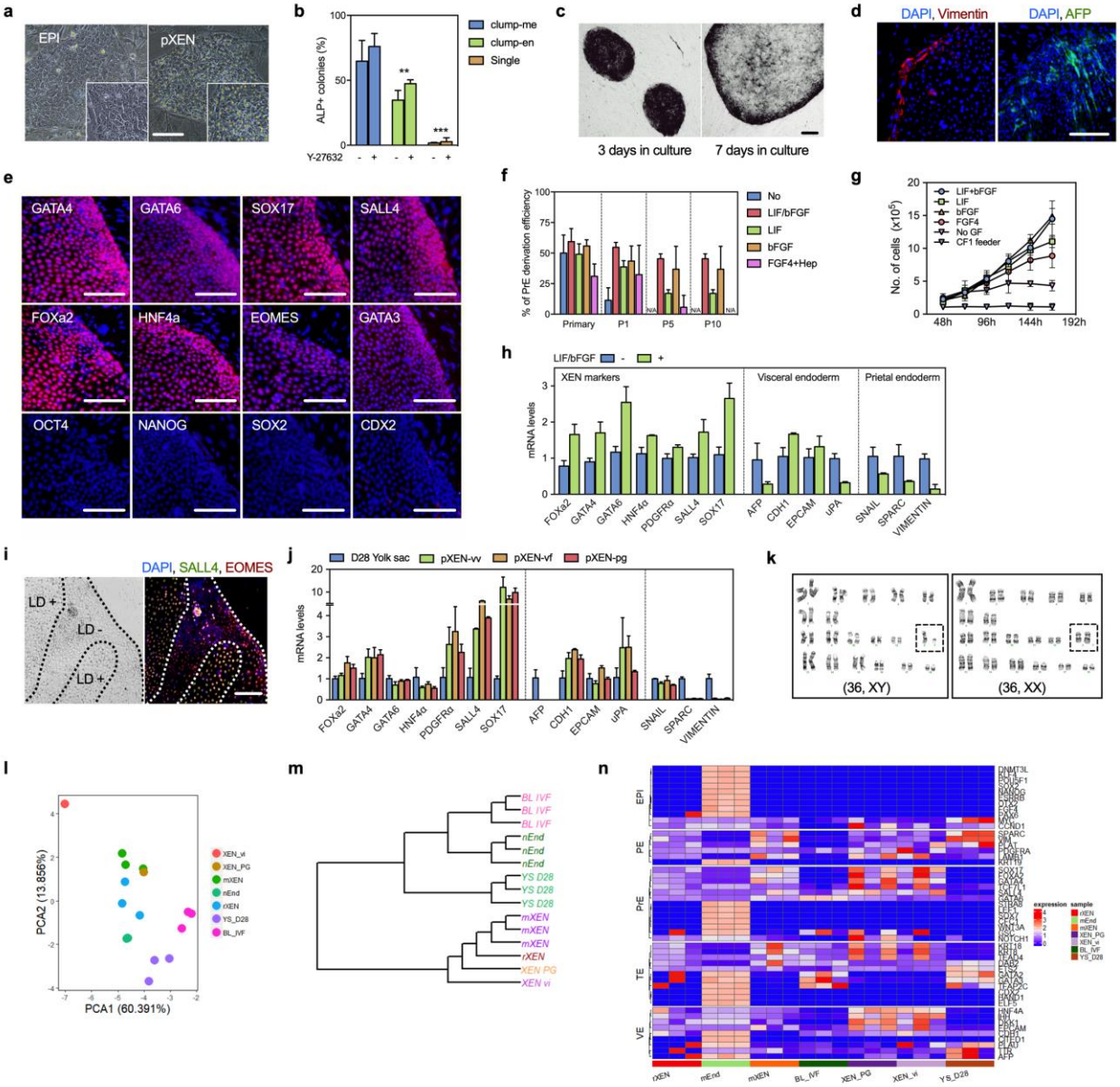

Figure 3

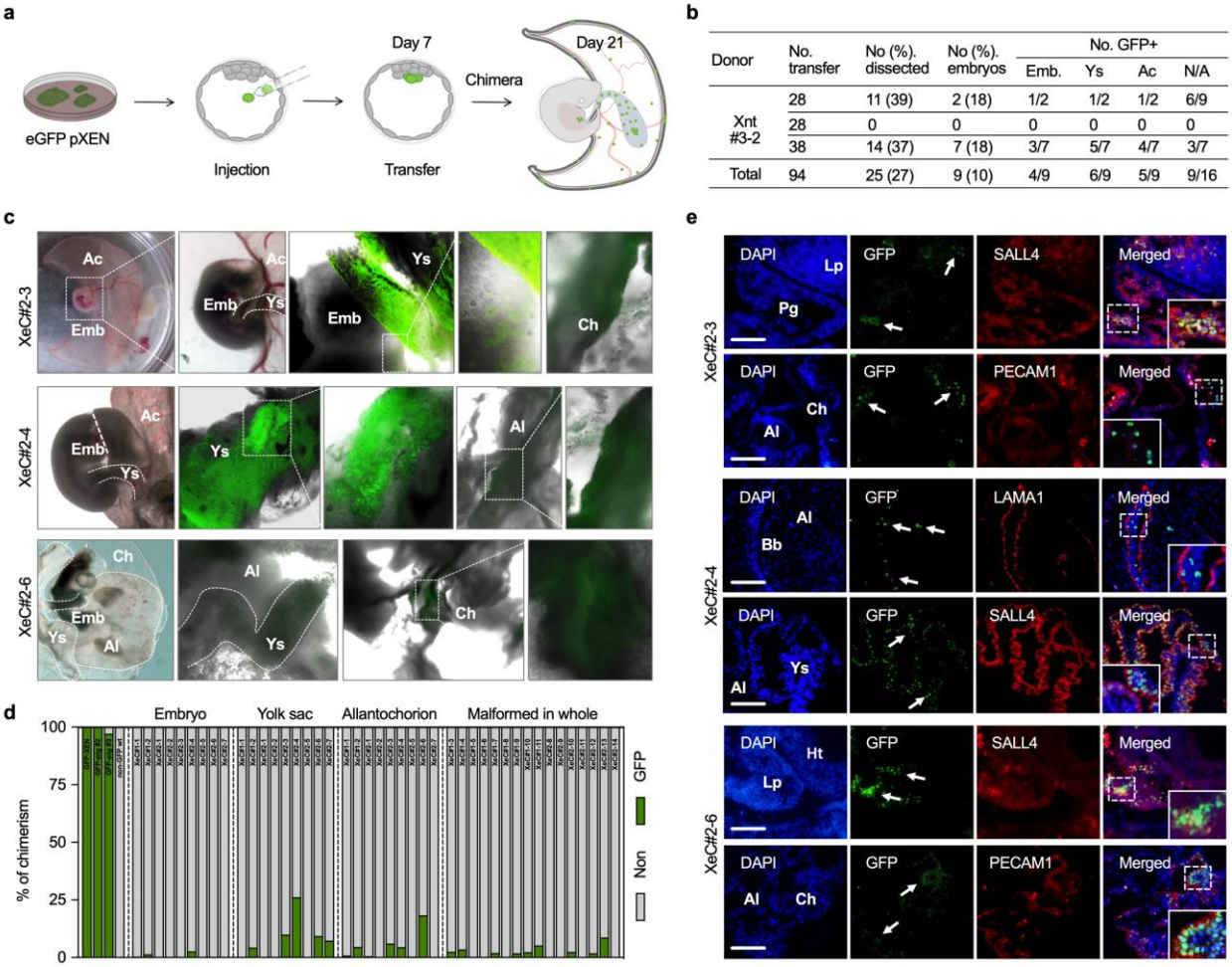

Donor	No. transfer	No (%). dissected	No (%). embryos	No. GFP+			
				Emb.	Ys	Ac	N/A
Xnt #3-2	28	11 (39)	2 (18)	1/2	1/2	1/2	6/9
	28	0	0	0	0	0	0
	38	14 (37)	7 (18)	3/7	5/7	4/7	3/7
Total	94	25 (27)	9 (10)	4/9	6/9	5/9	9/16

Figure 4

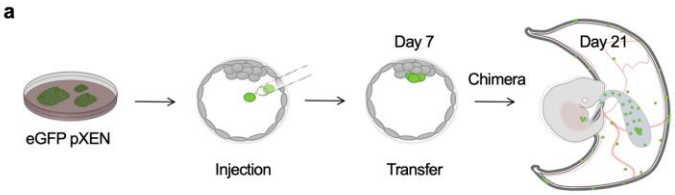

b

Donor	No. transfer	No (%). dissected	No (%). embryos	No. GFP+			
				Emb.	Ys	Ac	N/A
Xnt #3-2	28	11 (39)	2 (18)	1/2	1/2	1/2	6/9
	28	0	0	0	0	0	0
	38	14 (37)	7 (18)	3/7	5/7	4/7	3/7
Total	94	25 (27)	9 (10)	4/9	6/9	5/9	9/16